BMC Medical Imaging

RESEARCH

Open Access

Deep learning model for the automated detection and classification of central canal and neural foraminal stenosis upon cervical spine magnetic resonance imaging

Enlong Zhang[1†], Meiyi Yao[2†], Yuan Li[1†], Qizheng Wang[1†], Xinhang Song[2], Yongye Chen[1], Ke Liu[1], Weili Zhao[1], Xiaoying Xing[1], Yan Zhou[1], Fanyu Meng[2], Hanqiang Ouyang[3], Gongwei Chen[2], Liang Jiang[3], Ning Lang[1*], Shuqiang Jiang[2*] and Huishu Yuan[1*]

Abstract

Background A deep learning (DL) model that can automatically detect and classify cervical canal and neural foraminal stenosis using cervical spine magnetic resonance imaging (MRI) can improve diagnostic accuracy and efficiency.

Methods A method comprising region-of-interest (ROI) detection and cascade prediction was formulated for diagnosing cervical spinal stenosis based on a DL model. First, three part-specific convolutional neural networks were employed to detect the ROIs in different parts of the cervical MR images. Cascade prediction of the stenosis categories was subsequently performed to record the stenosis level and position on each patient slice. Finally, the results were combined to obtain a patient-level diagnostic report. Performance was evaluated based on the accuracy (ACC), area under the curve (AUC), sensitivity, specificity, F1 Score, diagnosis time of the DL model, and recall rate for ROI detection localization.

Results The average recall rate of the ROI localization was 89.3% (neural foramen) and 99.7% (central canal) under the five-fold cross-validation of the DL model. In the dichotomous classification (normal or mild vs. moderate or severe), the ACC and AUC of the DL model were comparable to those of the radiologists, and the F1 score (84.8%) of the DL model was slightly higher than that of the radiologists (83.8%) for the central canal. Diagnosing whether the central

†Enlong Zhang, Meiyi Yao, Yuan Li and Qizheng Wang contributed equally to this work.

*Correspondence:
Ning Lang
langning800129@126.com
Shuqiang Jiang
sqjiang@ict.ac.cn
Huishu Yuan
huishuy@sina.com
Full list of author information is available at the end of the article

canal or neural foramen of a slice is narrowed in the cervical MRI scan required an average of 15 and 0.098 s for the radiologists and DL model, respectively.

Conclusions The DL model demonstrated comparable performance with subspecialist radiologists for the detection and classification of central canal and neural foraminal stenosis on cervical spine MRI. Moreover, the DL model demonstrated significant timesaving ability.

Keywords Deep learning, MRI, Cervical spinal stenosis, Convolutional neural network

Background

Cervical spinal stenosis (CSS), which is an abnormal stenosis of the cervical canal [1], may lead to changes in the cervical spinal cord function and cervical radiculopathy [2]. CSS can affect the central and neural foraminal canals. Cervical spinal canal stenosis (SCS) is defined as abnormal narrowing of the central canal resulting in spinal cord compression and associated clinical symptoms. Second, neural foramen stenosis (NFS) can lead to compression of the nerve roots because they exit the spinal cord through the neural foramen. Moreover, herniated discs, facet joint and ligament hypertrophy, and vertebral instability can cause NFS.

Cervical degenerative changes can lead to significant clinical morbidity, resulting in cervical SCS and NFS [3]. Patients with CSS have various clinical manifestations that often make early diagnosis challenging [4]. However, early treatment is essential for monitoring the disease course and preventing persistent deterioration [5]. Furthermore, the function of the patient at the time of diagnosis and underlying etiology determine the prognosis of patients with CSS [6].

Conventional cervical magnetic resonance imaging (MRI), which is a valuable tool for CSS assessment, can accurately assess the degree of SCS and NFS and plays an important role in determining the appropriate treatment; however, describing this detailed information in a report can be repetitive and time-consuming. A fast and reliable imaging technique is warranted to diagnose and quantify different degrees of CSS spinal cord compression. Deep learning (DL) can improve the productivity and consistency of diagnostic reporting. DL has also been successfully applied to automatic vertebral segmentation in spinal imaging [7, 8].

Most studies on the automated analysis of degenerative spine imaging have focused on the lumbar spine. For example, DL in the lumbar spine and MRI have been used for vertebral segmentation and intervertebral disc degeneration grading [9–11], and a multitask architecture (denoted as SpineNet) has been developed for the automated classification of lumbar central canal stenosis and other spinal conditions. A binary classification (present or absent) has been employed for central canal stenosis. Lu et al. [12] developed a DL algorithm for grading lumbar spinal stenosis at the central canal and neural foramina without a predefined grading system. Recently, researchers have used the DL model to automatically detect and classify central canal, lateral recess, and neural foraminal stenoses of the lumbar spine [13, 14]. However, relatively few MRI studies have reported on cervical spondylosis. Merali et al. developed a convolutional neural network (CNN) model to detect cervical spinal cord compression in patients with degenerative cervical myelopathy using MRI scans. The results revealed that the heterogeneous group achieved higher model performance, with an area under the curve (AUC) of 0.94 [15]. Ma et al. developed a DL model based on MRI for cervical spinal cord compression in patients with cervical disc degenerative diseases and traumatic spinal cord injuries [16].

To our knowledge, no DL model has been developed to assess the stenosis in two regions-of-interest (ROIs) along the cervical spine. Thus, such a model can serve as an accurate and reliable diagnostic tool for CSS. In addition, the performance of traditional DL methods is unsatisfactory, and traditional CNNs have several drawbacks [17]. To address this problem, novel algorithms capable of powerful processing for object detection have been proposed. An example of such an algorithm is Faster R-CNN [18], which has better accuracy and detection speed. Faster R-CNN may improve the possibility of diagnosing lesions using cervical MRI.

Therefore, we aimed to develop a DL model (Faster R-CNN) to automatically detect and classify central canal and neural foraminal stenoses in the cervical spine using axial T2-weighted MRI in this study.

Methods

The study design was approved by the appropriate ethics review board, which waived the requirement for informed consent owing to the retrospective nature of the study.

Patient datasets

Patients with imaging-diagnosed degeneration between January 2016 and December 2018 were selected from the radiological reporting system of our hospital's cervical spine MRI database. In total, 796 patients (mean age ± standard deviation, 51 years ± 10.06; men: 495, 63.57%) were evaluated. Adult patients (>18 years old)

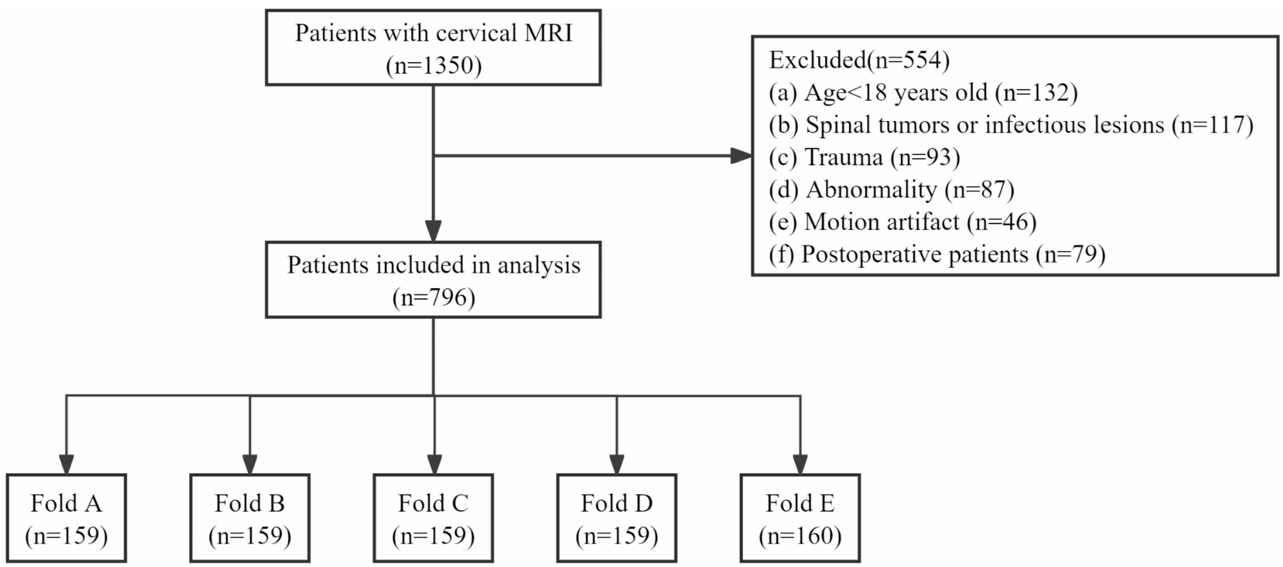

Fig. 1 Flowchart of the study population

Table 1 Details on the magnetic resonance imaging scanners and sequences

MRI scanners	Sequences	FOV (mm^2)	Slice thickness (mm)	TR(ms)/TE (ms)	Flip angle
GE 1.5 T	T2* MERGE	200×150	4	433.1/5.5	20
GE 3.0 T (HDXT)	T2 FRFSE	256×128	4	552.9/12.0	20
Siemens 3.0 T(Prisma)	T2 FRFSE	190×140	4	400.0/17.0	20
United Imaging 3.0 T					
uMR780	GRE	200×150	4	592.1/13.45	20
uMR880	GRE	200×150	4	608/13.33	20

MRI magnetic resonance imaging, *FOV* field of view, *TR* repetition time, *TE* echo time, *MERGE* multiple echo recombined gradient echo, *FRFSE* fast recovery fast spin echo, *GRE* gradient recalled echo

were included in the study. Patients were excluded from the study if they had undergone instrumentation or presented with other conditions, such as spinal tumors, infections, trauma, or scoliosis. Additionally, MRI data with significant motion artifacts were excluded to ensure acceptable quality and reliability of the imaging analysis (Fig. 1).

MRI

Cervical spine MRI studies were performed using different MRI scanners (GE 1.5- and 3.0-T platforms; Siemens 3.0 T platforms; United Imaging 3.0 T platforms), with the same sequences and standard phased-array surface coils. Table 1 provides details of the MRI scanners and sequences.

Data set labeling

The data were desensitized before use to ensure that patient information was not leaked. The raw data in standard Digital Imaging and Communications in Medicine (DICOM) format was used to ensure lossless data transmission. All personnel involved in labeling were required to receive unified training and pass a training assessment prior to their qualification. All data were annotated by four junior radiologists with ≥3 years of imaging experience. After the data labeling was completed, it was reviewed and confirmed by two musculoskeletal radiology experts with >20 years of experience, and the consistent opinions of the two experts were considered the diagnostic reference label. Each radiologist was blinded to the patient demographics and clinical history. Using open-source annotation software, bounding boxes were drawn to segment the ROIs (central canal and neural foramina) at and between each cervical disc level. When drawing each bounding box, the annotating radiologist classified the cervical stenosis. The grading system for the severity of stenosis was based on transverse T2 weighted imaging (WI) findings and classified according to the following criteria: Grading system for SCS: Grade 0, no stenosis; Grade 1, Mild stenosis with less than 50% obstruction; Grade 2, Moderate stenosis characterized by spinal canal narrowing with spinal cord deformation but without signal changes within the spinal cord; and Grade 3, Severe stenosis with narrowing accompanied by high signal intensity within the spinal cord. Grading system for NFS: Grade 0, no stenosis; Grade 1, Mild stenosis, where the fat surrounding the nerve root is obstructed by <50% of the nerve root circumference, with no morphological changes to the nerve root; Grade 2, Moderate stenosis with obstruction of the fat surrounding the nerve root

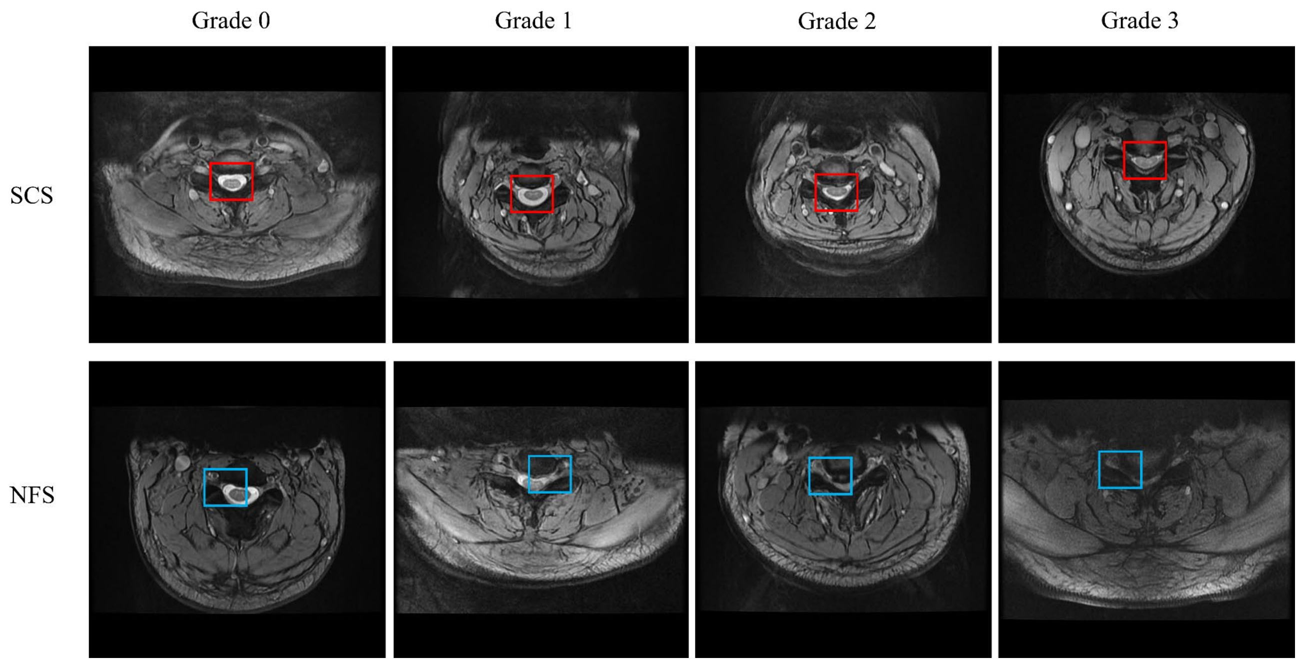

Fig. 2 Classification diagram of spinal canal stenosis and neural foramen stenosis

Table 2 Evaluation of the severity of cervical spinal stenosis by using three-tiered grading system

Degree of spinal stenosis	Neural foramen	Central canal
Normal	2158	1576
Mild	2350	1263
Moderate	2134	654
Severe	734	195
Total	7376	3688

exceeding 50% of the nerve root circumference, without morphological changes to the nerve root; and Grade 3, Severe stenosis manifesting as collapse of the nerve root. Grading was performed using well-established criteria for CSS at the central canal and neural foramina [19–22] (Fig. 2) (Table 2). Four junior radiologists independently evaluated the MRI images to determine the presence or absence of spinal stenosis. The start and end times of each physician's evaluation of each image were also recorded.

Development of the DL model

A method for diagnosing cervical spinal stenosis was proposed based on the DL model (Faster R-CNN) [18], consisting of an ROI detection module and cascade classification prediction. First, three types of CNNs were used to detect the ROIs in different parts of the cervical MR images (the left neural foramen, right neural foramen, and central canal). The image features of the ROIs extracted by the CNNs were then fed to the full connection layer (normal, mild, moderate, and severe) for classification. Cascade classification was subsequently performed to predict the CSS status of each patient slice. Finally, the results were combined to obtain a patient-level diagnostic report (Fig. 3). The overall cascading process design was seamlessly integrated with the processing workflow of the DL models.

After experimental comparison, the optimizer for the DL models used Stochastic Gradient Descent with an initial learning rate of 0.02 Each model was trained for 50 epochs, and the learning rate adjustment strategy was selected as StepLR, which was updated every 5 epochs, with a gamma of 0.5. The loss function is a composite of ROI detection, which was calculated using the Intersection over Union (IoU) of the ground truth and predicted bounding boxes, and classification losses, which was calculated using a four-class focal loss function for classification.

Statistical analysis

All the statistical analyses were performed using SPSS version 23 software (IBM Corp., Armonk, NY, USA). Continuous variables are expressed as mean ± standard deviation, while categorical variables are expressed as frequencies and ratios. Cohen's κ test was performed to determine the consistency between the DL model results and junior radiologist annotated results, providing Cohen's κ coefficient and its 95% confidence interval. The DL model was developed in Python (version 3.8) and PyTorch (version 1.8.1).

The performance was evaluated based on the accuracy (ACC), area under the curve (AUC), sensitivity, specificity, F1 score, diagnosis time used for classification, and

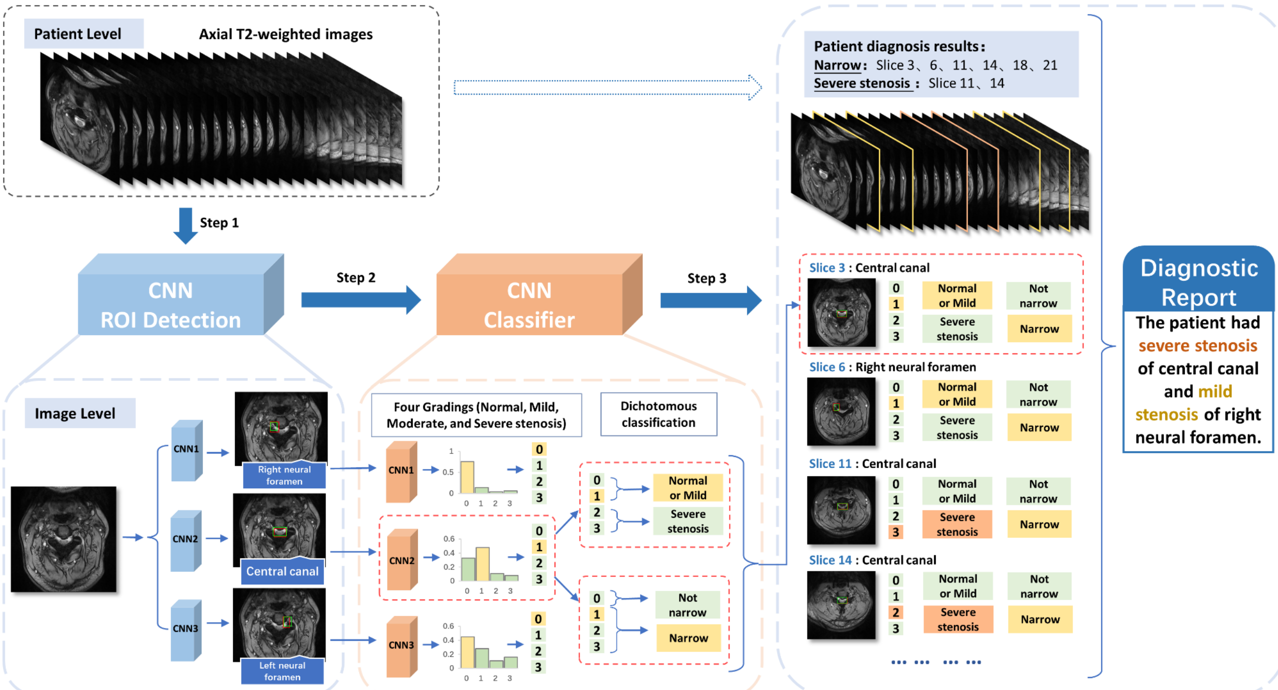

Fig. 3 Flowchart of deep learning models. Flowchart of deep learning models for automated detection and classification of central canal and neural foraminal stenosis upon cervical spine magnetic resonance imaging

Table 3 Region-of-interest recall rate

Recall rate (IoU > 0.5)	Neural foramen	Central canal
DL model a	90.7%	99.7%
DL model b	87.7%	99.9%
DL model c	90.4%	99.9%
DL model d	90.0%	99.3%
DL model e	87.8%	99.9%
Average	**89.3%**	**99.7%**

IoU intersection over union, *DL* deep learning

recall rate for ROI detection localization. To determine the presence of a significant difference between the AUC values, we used the DeLong test. IoU was used to measure the degree of overlap between the predicted and annotated areas. IoU > 0.5 is considered a reasonable prediction result in most general cases, and the positioning of the ROIs is accurate. To ensure complete data utilization and avoid the impact of an uneven data distribution, a similar five-fold cross-validation was adopted to test the evaluation metrics, which can also verify the robustness of the DL model. All the test results were averaged over five random partitions that covered each other. One was selected as the test set for each division, and the other four were selected as the training set. All evaluation metrics were calculated as the average of five different divisions.

Results

ROI detection

Considering IoU > 0.5 as the threshold, the average recall rate of ROIs localization was 89.3% (neural foramen) and 99.7% (central canal) under the five-fold cross-validation of our DL model (Table 3).

Classification of the test results

The DL model demonstrated exceptional efficiency in diagnosing the narrowing of the central canal or neural foramen. The DL model processed each MRI slice in 0.098 s, which was significantly faster than the radiologists (average time of 15 s).

In the dichotomous classification (normal or mild vs. moderate or severe), the average accuracy of the five-fold cross-validation of the DL model was 0.880 and 0.827 in the neural foramen and central canal, respectively, which were comparable to the radiologists' accuracies of 0.909 and 0.842, with a difference of 0.029 and 0.015, respectively (Table 4).

For the neural foramen, the AUC for the DL model was 0.890 (95% confidence interval [CI]: 0.882–0.8979), which was slightly higher than that of the radiologists (0.838; 95% CI: 0.829–0.846) (*P<0.0001*, Delong's test) (Fig. 4). The sensitivities of the DL model and radiologist were 0.705 and 0.709, respectively, which were almost identical. The specificity of the DL model was as high as 0.927, which was comparable to that of a radiologist (0.966).

Table 4 Accuracy based on the dichotomous classification of the neural foramen and central canal (normal or mild vs. moderate or severe)

Parameter		Neural foramen	Central canal
Split a	DL model a	0.864	0.799
	radiologist	0.899	0.838
Split b	DL model b	0.891	0.839
	radiologist	0.915	0.850
Split c	DL model c	0.874	0.820
	radiologist	0.908	0.818
Split d	DL model d	0.887	0.842
	radiologist	0.906	0.842
Split e	DL model e	0.886	0.836
	radiologist	0.916	0.864
Average	**DL model**	**0.880**	**0.827**
	radiologist	**0.909**	**0.842**

DL deep learning

Table 5 Comparison of performance metrics

Metric	Parameter	Neural foramen	Central canal
AUC (95% CI)	DL model	0.890 (0.882, 0.897)	0.876 (0.865, 0.886)
	radiologist	0.838 (0.829, 0.846)	0.859 (0.848, 0.870)
Delong test		$Z=8.095$ $P<0.0001$	$Z=2.641$ $P=0.0083$
Sensitivity	DL model	0.705	0.835
	radiologist	0.709	0.725
Specificity	DL model	0.927	0.819
	radiologist	0.966	0.993
Precision	DL model	0.758	0.839
	radiologist	0.859	0.993
F1 score	DL model	0.718	0.848
	radiologist	0.777	0.838

AUC area under the curve, CI confidence interval, *DL* deep learning

The test results for the central canal differed from those of the neural foramen (Table 5). The mean sensitivity of the DL model (0.835) was 0.11 higher than that of the radiologists (0.725), and although its specificity was lower (0.819 compared to 0.993), the overall AUC (0.876, 95% CI: 0.865, 0.886) was still comparable to the radiologists' performance (0.859, 95% CI: 0.848, 0.870) or even slightly higher ($P=0.0083$, Delong test) (Fig. 5). The F1 score of the DL model was 0.848, which was slightly higher than that of the radiologists (0.838).

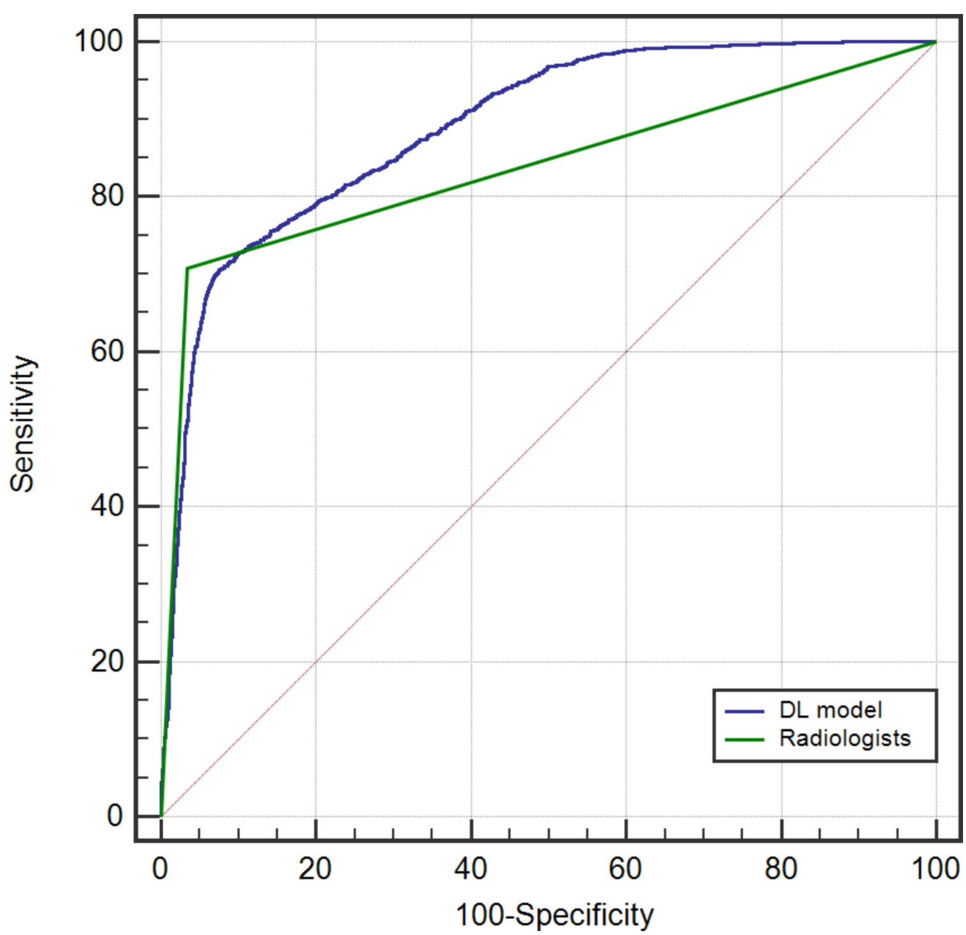

Fig. 4 Receiver operating characteristic curve on the dichotomous classification of the neural foramen (Normal or mild vs. moderate or severe)

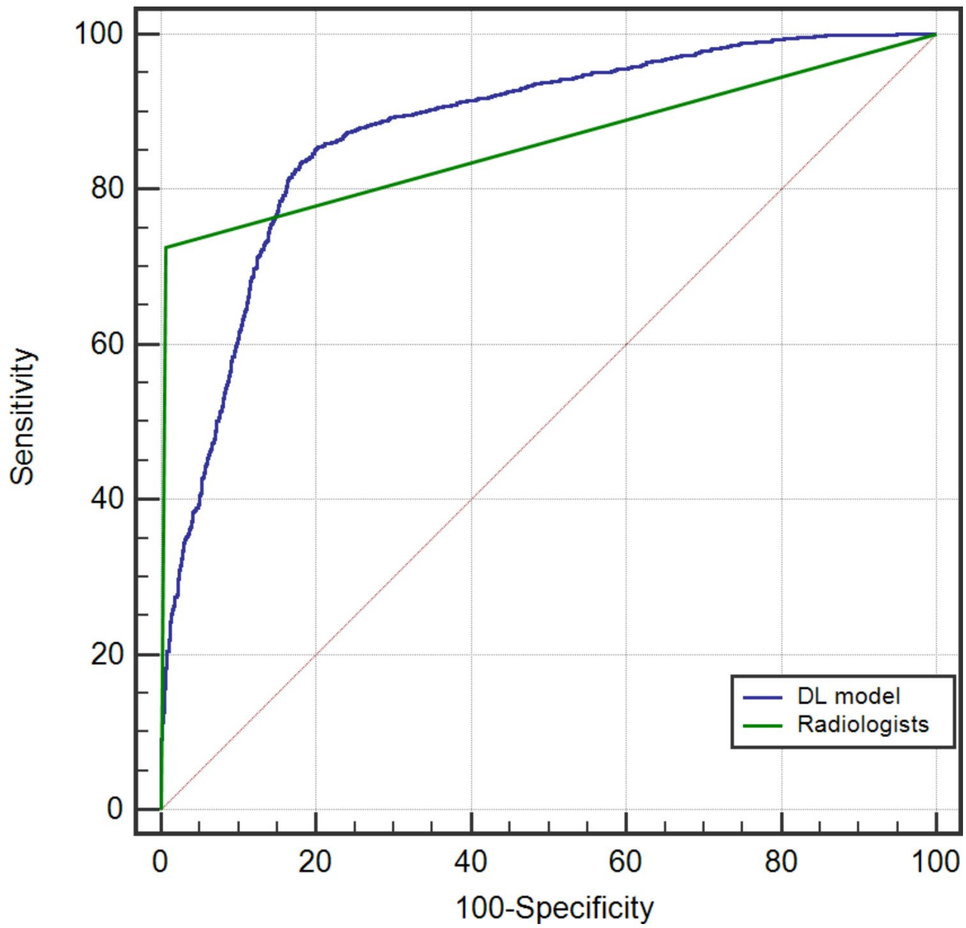

Fig. 5 Receiver operating characteristic curve on the dichotomous classification of central canal (Normal or mild vs. moderate or severe)

Table 6 Cohen's κ test

	Neural foramen	Central canal
DL model (95% confidence interval)	0.644 (0.630, 0.657)	0.649 (0.624, 0.674)
Radiologist (95% confidence interval)	0.725 (0.714, 0.736)	0.692 (0.670, 0.714)

DL deep learning

For the neural foramen (N) and central canal (C) classification, the DL model agreement (N: Cohen's $\kappa=0.644$; 95% CI: 0.630, 0.657; C: Cohen's $\kappa=0.649$, 95% CI: 0.624, 0.674; $P<0.001$; respectively) was reduced compared with that of the radiologist (N: Cohen's $\kappa=0.725$; 95% CI: 0.714, 0.736; $P<0$ 0.001; C: Cohen's $\kappa=0.692$; 95% CI: 0.670, 0.714; $P<0.001$; respectively) (Table 6).

Discussion

Cervical spine MRI, which is an essential tool for evaluating CSS, can accurately assess SCS and NFS. Clinical history and examination are regarded the most important diagnostic tools for patients with suspected CSS; however, spinal neuroimaging is critical for confirmation and further refinement of the diagnosis. The CSS grade is also important, and the degree of stenosis in each region plays an important role in determining appropriate treatment. According to the grading system reported in previous research [19–22], all the participants were classified into four grades of SCS and NFS. The degrees of SCS and NFS play an important role in determining appropriate treatment. Grade 3 SCS is associated with adverse clinical outcomes and decreased response to decompression surgery [23–25]. Takahashi et al. [26] revealed the severity of spinal canal distortion with cord compression to be directly proportional to the severity of clinical impairment, and that grade 3 SCS had a poorer prognosis. Sun et al. [27] demonstrated the NFS grade to be an important factor in determining additional uncinate process resection in anterior cervical discectomy and fusion. However, relaying this information to physicians to assess serial MR images for classifying the CSS grades in detail in a report can be repetitive and time-consuming. Moreover, opinions regarding the diagnosis of the grade of CSS may vary among physicians.

The DL model can be used to automatically detect and classify SCS and NFS on cervical spine MRI, which can improve the accuracy and efficiency of diagnosis and save the time of physicians. In this study, a CSS method was proposed based on the DL model comprising ROI detection and cascade prediction using MRI. Cascade classification consists of four levels: patient-level image input to individual image processing, individual images to distinct ROI analysis, single ROI areas to quadruple classification of stenosis, quadruple classification of stenosis to optional binary classification, and finally, synthesizing the results into a patient-level diagnostic outcome. The overall cascading process design was seamlessly integrated with the processing workflow of the DL models, utilizing data that included MR axial images and annotations of ROIs. In the dichotomous classification (normal or mild vs. moderate or severe), the ACC and AUC of the DL model were comparable to those of the radiologists, and the F1 score of the DL model was slightly higher than that of the radiologists for the central canal. The IoU of the ROI detection revealed that it could accurately locate the central canal and neural foramen. Diagnosing whether a slice's central canal or neural foramen is narrowed by cervical MRI sequences required an average of 15 and 0.098 s by the radiologists and the DL model, respectively (using Intel(R) Xeon(R) CPU E5-2620 v3 @ 2.40 GHz as CPU and GeForce GTX TITAN X GPU). This significant time difference not only demonstrates the superior advantage of the DL model in terms of diagnostic efficiency but also provides data support for possible workflow improvements in future clinical applications. To our knowledge, no prior study has assessed the automated detection and classification of central canal and neural foramen stenoses.

Faster R-CNN was proposed as a new algorithm with high processing speeds for object detection in 2015. In addition, numerical experiments have demonstrated that Faster R-CNN combined with novel CNN models has better recognition performance than several traditional detection methods [28]. Most studies on the automated analysis of spinal stenosis have focused on the lumbar spine. Few studies have applied DL models to cervical spine imaging. Ma et al. implemented Faster R-CNN to detect lesions in cervical MR images. The mean average precision for the Faster R-CNN with ResNet-50 and VGG-16 was 88.6 and 72.3%, respectively, and the average time of diagnosis was 0.22 and 0.24 s/image, respectively. The experimental results revealed that Faster R-CNN improved the possibility of diagnosing lesions using cervical MRI. Merali et al. developed a DL model to detect cervical spinal cord compression in 289 patients with degenerative cervical myelopathy on MRI scans and achieved a high performance on the holdout dataset with an AUC of 0.94, sensitivity of 0.88, specificity of 0.89, and F1 score of 0.82 [15]. Our DL model not only demonstrated high accuracy, but also a short average diagnostic time and good diagnostic performance. Moreover, the size of the dataset used was larger, and the robustness test of the algorithm demonstrated better generalization performance. In addition, few previous studies have evaluated the automatic detection and classification of CSS, and our DL model can provide more flexible and detailed diagnostic results according to the clinical needs.

This study has certain limitations. First, the dataset used was limited to the imaging system at our hospital. Although this method can ensure uniformity of data, compared with other databases, the amount of data is insufficient, and the scalability is poor. Future studies should focus on multicenter data. Second, we focused only on axial T2WI as the target of grading for CSS evaluation. However, in the central canal stenosis grading system, we adapted selected sagittal T2WI images and the cervical neural foraminal stenosis grading system selected oblique sagittal images. Moreover, axial T2WI was the single most important sequence for evaluating CSS. In addition, a previous study found that both axial and oblique sagittal images supported strong interobserver reliability for assessing the concordance between the MRI grades of cervical neural foraminal stenosis [29]. Therefore, evaluating stenosis of the spinal canal and foramina in the axial position instead of the sagittal and oblique sagittal positions is considered feasible. Lastly, manual labeling of images by radiologists is considered the most accurate method for training models; however, this is a labor-intensive method and limits the number of MRI cervical spine studies available for training.

Conclusions

We demonstrated that our DL model is reliable and can be used to quickly assess CSS using MRI scans. In clinical practice, the diagnosis of CSS relies on the subjective opinion of a reporting radiologist. Our DL model demonstrated comparable performance to subspecialist radiologists for the detection and classification of central canal and neural foraminal stenoses on cervical spine MRI scans; moreover, the DL model demonstrated significant time saving ability. Thus, this method can provide a reference diagnosis for CSS and can be assessed for the longitudinal follow-up of CSS upon MRI.

Abbreviations

ACC	Accuracy
AUC	Area under the curve
CI	Confidence interval
CNN	Convolutional neural network
CSS	Cervical spinal stenosis
DL	Deep learning
IoU	Intersection over Union
MRI	Magnetic resonance imaging
NFS	Neural foramen stenosis
ROI	Region-of-interest

SCS Spinal canal stenosis
WI Weighted imaging

Author contributions
Design of the work: NL, SQJ, HSY.Acquisition of data: QZW, YYC, KL, WLZ, XYX, YZ, HQO, LJ.Interpretation of data: MYY, FYM, GWC, XHS.Drafting/Critical revision: ELZ, MYY, YL, NL, XHS.Final approval: NL, HSY.

Funding
This research was funded by Beijing Natural Science Foundation (Z190020);National Natural Science Foundation of China (82371921, 81971578, 62032022, 61902378, 81871326, 81901791, 82102638); Clinical Medicine Plus X-Young Scholars Project, Peking University, the Fundamental Research Funds for the Central Universities (PKU2021LCXQ005); Peking University Third Hospital Clinical Key Project (BYSYZD2021040). The funding bodies played no role in the design of the study and collection, analysis, and interpretation of data and in writing the manuscript.

Data availability
The datasets used and/or analysed during the current study are available from the corresponding author on reasonable request.

Declarations

Ethics approval and consent to participate
The methods were performed in accordance with relevant guidelines and regulations and approved by Peking University Third Hospital Medical Science Research Ethic Committee, which waived the requirement of informed consent due to the retrospective nature of the study.

Consent for publication
Not Applicable.

Competing interests
The authors declare no competing interests.

Author details
[1]Department of Radiology, Peking University Third Hospital, 49 North Garden Road, Haidian District, Beijing 100191, PR China
[2]Institute of Computing Technology, Chinese Academy of Sciences, Beijing, China
[3]Department of Orthopaedics, Engineering Research Center of Bone and Joint Precision Medicine, Beijing Key Laboratory of Spinal Disease Research, Peking University Third Hospital, 49 North Garden Road, Haidian District, Beijing 100191, China

Received: 18 September 2023 / Accepted: 4 November 2024
Published online: 26 November 2024

References
1. Lebl DR, Bono CM. Update on the diagnosis and management of cervical spondylotic myelopathy. J Am Acad Orthop Surg. 2015;23(11):648–60.
2. Martin AR, Tadokoro N, Tetreault L, et al. Imaging evaluation of degenerative cervical myelopathy: current state of the art and future directions. Neurosurg Clin N Am. 2018;29(1):33–45.
3. Tracy JA, Bartleson JD. Cervical spondylotic myelopathy. Neurologist. 2010;16(3):176–87.
4. Behrbalk E, Salame K, Regev GJ, et al. Delayed diagnosis of cervical spondylotic myelopathy by primary care physicians. Neurosurg Focus. 2013;35(1):E1.
5. Edwards CC 2nd, Riew KD, Anderson PA, Hilibrand AS, Vaccaro AF. Cervical myelopathy. Current diagnostic and treatment strategies. Spine J. 2003;3(1):68–81.
6. Tetreault LA, Cote P, Kopjar B, et al. A clinical prediction model to assess surgical outcome in patients with cervical spondylotic myelopathy: internal and external validations using the prospective multicenter AOSpine North American and international datasets of 743 patients. Spine J. 2015;15(3):388–97.
7. Michopoulou SK, Costaridou L, Panagiotopoulos E, et al. Atlas-based segmentation of degenerated lumbar intervertebral discs from MR images of the spine. IEEE Trans Biomed Eng. 2009;56(9):2225–31.
8. Berg-Johansen B, Han M, Fields AJ, et al. Cartilage endplate thickness variation measured by Ultrashort Echo-Time MRI is Associated with adjacent disc degeneration. Spine (Phila Pa 1976). 2018;43(10):E592–600.
9. Zhou Y, Liu Y, Chen Q, Gu G, Sui X. Automatic lumbar MRI detection and identification based on deep learning. J Digit Imaging. 2019;32(3):513–20.
10. Jamaludin A, Lootus M, Kadir T, et al. ISSLS Prize in Bioengineering Science 2017: automation of reading of radiological features from magnetic resonance images (MRIs) of the lumbar spine without human intervention is comparable with an expert radiologist. Eur Spine J. 2017;26(5):1374–83.
11. Jamaludin A, Kadir T, Zisserman A, SpineNet. Automated classification and evidence visualization in spinal MRIs. Med Image Anal. 2017;41:63–73.
12. Lu J-T, Pedemonte S, Bizzo B et al. DeepSPINE: Automated Lumbar Vertebral Segmentation, Disc-level Designation, and Spinal Stenosis Grading Using Deep Learning2018 July 01, 2018:[arXiv:1807.10215 p.]. https://ui.adsabs.harvard.edu/abs/2018arXiv180710215L
13. Hallinan J, Zhu L, Yang K, et al. Deep learning model for automated detection and classification of Central Canal, lateral recess, and neural Foraminal stenosis at lumbar spine MRI. Radiology. 2021;300(1):130–8.
14. Hayashi D. Deep learning for lumbar spine MRI reporting: a welcome Tool for radiologists. Radiology. 2021;300(1):139–40.
15. Merali Z, Wang JZ, Badhiwala JH, et al. A deep learning model for detection of cervical spinal cord compression in MRI scans. Sci Rep. 2021;11(1):10473.
16. Ma S, Huang Y, Che X, Gu R. Faster RCNN-based detection of cervical spinal cord injury and disc degeneration. J Appl Clin Med Phys. 2020;21(9):235–43.
17. Litjens G, Kooi T, Bejnordi BE, et al. A survey on deep learning in medical image analysis. Med Image Anal. 2017;42:60–88.
18. Ren S, He K, Girshick R, Sun J, Faster R-CNN. Towards real-time object detection with region proposal networks. IEEE Trans Pattern Anal Mach Intell. 2017;39(6):1137–49.
19. Kang Y, Lee JW, Koh YH, et al. New MRI grading system for the cervical canal stenosis. AJR Am J Roentgenol. 2011;197(1):W134–140.
20. Park HJ, Kim SS, Lee SY, et al. A practical MRI grading system for cervical foraminal stenosis based on oblique sagittal images. Br J Radiol. 2013;86(1025):20120515.
21. Kushchayev SV, Glushko T, Jarraya M, et al. ABCs of the degenerative spine. Insights Imaging. 2018;9(2):253–74.
22. Hutchins J, Hebelka H, Lagerstrand K, et al. A systematic review of validated classification systems for cervical and lumbar spinal foraminal stenosis based on magnetic resonance imaging. Eur Spine J. 2022;31(6):1358–69.
23. Sampath P, Bendebba M, Davis JD, Ducker TB. Outcome of patients treated for cervical myelopathy. A prospective, multicenter study with independent clinical review. Spine (Phila Pa 1976). 2000;25(6):670–6.
24. Meyer F, Borm W, Thome C. Degenerative cervical spinal stenosis: current strategies in diagnosis and treatment. Dtsch Arztebl Int. 2008;105(20):366–72.
25. Kadanka Z, Mares M, Bednanik J, et al. Approaches to spondylotic cervical myelopathy: conservative versus surgical results in a 3-year follow-up study. Spine (Phila Pa 1976). 2002;27(20):2205–10. discussion 2210 – 2201.
26. Takahashi M, Sakamoto Y, Miyawaki M, Bussaka H. Increased MR signal intensity secondary to chronic cervical cord compression. Neuroradiology. 1987;29(6):550–6.
27. Sun B, Xu C, Zhang Y, et al. Intervertebral Foramen Width is an important factor in deciding additional uncinate process resection in ACDF-a retrospective study. Front Surg. 2021;8:626344.
28. He K, Sun J. Convolutional Neural Networks at Constrained Time Cost. 2014.
29. Kim W, Ahn KS, Kang CH, Kang WY, Yang KS. Comparison of MRI grading for cervical neural foraminal stenosis based on axial and oblique sagittal images: concordance and reliability study. Clin Imaging. 2017;43:165–9.

Publisher's note